Photodiagnosis and Photodynamic Therapy 28 (2019) 10–17

Contents lists available at ScienceDirect

Photodiagnosis and Photodynamic Therapy

journal homepage: www.elsevier.com/locate/pdpdt

Photoirradiation after aminolevulinic acid treatment suppresses cancer cell proliferation through the HO-1/p21 pathway

Taku Nakayama[a,b], Tatsuya Kobayashi[a], Otsuka Shimpei[a], Hideo Fukuhara[b,c], Tsutomu Namikawa[b,d], Keiji Inoue[b,c], Kazuhiro Hanazaki[b,d], Kiwamu Takahashi[e], Motowo Nakajima[e], Tohru Tanaka[e], Shun-ichiro Ogura[a,b,*]

[a] Department of Bioengineering, School of Life Science and Technology, Tokyo Institute of Technology, Japan
[b] Center for Photodynamic Medicine, Kochi Medical School, Japan
[c] Department of Urology, Kochi Medical School, Japan
[d] Department of Surgery I, Kochi Medical School, Japan
[e] SBI Pharmaceuticals Co., Ltd., Japan

ARTICLE INFO

Keywords:
Cancer
5-aminolevulinic acid
Photodynamic therapy
Cell cycle
p21

ABSTRACT

Background: Photodynamic therapy (PDT) and diagnosis (PDD) using 5-aminolevulinic acid (ALA) to control the production of an intracellular photosensitizer, protoporphyrin IX (PpIX), are in common clinical use. Although various studies have been published regarding cell death analysis after photoirradiation by ALA-PDT, the changes in gene expressions induced by it are yet unclear. Here, we focused on studying gene expression and cell proliferation changes in cancer cells that survive photoirradiation.

Methods: HEK293 human embryonic kidney cells, MKN45 human gastric cells, and PC-3 human prostate cancer cells were selected for this research. Cell viability was measured using trypan blue and MTT assays. ALA-PDT experiments were performed using a calibrated LED irradiation module. Furthermore, mRNA and protein gene expression analysis were performed using our previously reported methods.

Results: mRNAs of PAI-1, HO-1, and p21 were upregulated after photoirradiation of HEK293, which was suppressed by N-acetyl-L-cysteine, a reactive oxygen species (ROS) scavenger. Primer array results in PC-3 cells and p21 and Ki-67 expression results in both PC-3 and MKN45 cells suggested that photoirradiation suppressed cell proliferation. Cell numbers post-photoirradiation revealed that the proliferation of surviving cells was suppressed in PC-3 and MKN45 cells.

Conclusion: ALA-PDD or ALA-PDT can result in rapid ROS-induced cell death and may decrease long-term recurrence rates through several pathways including the HO-1/p21 pathway.

1. Introduction

5-Aminolevulinic acid (ALA) is an amino acid that is a precursor in porphyrin biosynthesis in plants and animals. Porphyrin, which is biosynthesized from ALA, functions as an important cofactor in both plant and animal cells. Various metals are inserted into the porphyrin structure, and these metal porphyrins have several functions *in vivo*. For example, a magnesium ion inserted into porphyrin is an important component of chlorophyll, whereas an iron ion inserted into porphyrin is an important component of heme, which functions as the active site in various enzymes such as CYP450, catalase, and the electron transport chain complexes in mitochondria [1]. Protoporphyrin IX (PpIX) is a fluorophore with a maximum excitation and emission at approximately 405 nm and 635 nm, respectively. Metal free porphyrins, including PpIX, can function as photosensitizers. Furthermore, although the mechanism is yet unclear, various types of tumors accumulate PpIX after ALA treatment [2–4]. Therefore, ALA is used clinically for photodynamic diagnosis (ALA-PDD) and therapy (ALA-PDT) of tumors.

ALA-PDT is an effective and minimally invasive treatment for cancer. Moreover, several factors, for example light dose, ALA concentration, oxygen concentration, expression of porphyrin transporters, and cellular dormancy, have been reported to influence the efficacy of ALA-PDT [5–7]. Several reports have shown that PDT functions via two types of reactions. The type I reaction results in hydrogen or electron

* Corresponding author at: Department of Bioengineering, School of Life Science and Technology, Tokyo Institute of Technology, 4259 B47 Nagatsuta-cho, Midori-ku, Yokohama, 226-8501, Japan.
E-mail address: sogura@bio.titech.ac.jp (S.-i. Ogura).

https://doi.org/10.1016/j.pdpdt.2019.07.021
Received 5 June 2019; Received in revised form 9 July 2019; Accepted 26 July 2019
Available online 09 August 2019
1572-1000/

transfer between the photosensitizer and substrate to produce free radicals that react with oxygen to produce superoxide radical anions. In the type II reaction, singlet oxygen is produced through an energy transfer process between ground state oxygen and the excited photosensitizer during its return to its ground state. Therefore, ALA-PDT can exert its effects in numerous ways, for example, by generating reactive oxygen species (ROS) containing singlet oxygen that induces apoptosis, necrosis, and autophagic cell death [8–10]. This cell death pathway is rapid and is completed within a few days at most.

Our group at Kochi University performed the first urological clinical study regarding ALA-PDD in 2004 including 18 patients with bladder cancer [11]. Further, we conducted a study that reported a 93.4% sensitivity and 58.9% specificity in 210 patients with bladder cancer [12]. Until the end of 2018, ALA-PDD has been performed in 3653 patients with bladder cancer at 293 institutions in Japan. In contrast, ALA-PDT is not widely used in Japan; however, clinical studies are ongoing for several cancers.

Although numerous reports regarding cell death analysis after ALA-PDT have been published, the changes in gene expression in cells that survive photoirradiation remain unclear. Therefore, in this study, we focused on examining cell proliferation and the changes in gene expressions after photoirradiation.

2. Material & methods

2.1. Biochemicals

ALA hydrochloride was purchased from Cosmo Oil Co., Ltd. (Tokyo, Japan). We obtained the RPMI-1640 medium, antibiotic antimycotic solution (ABAM), and protease inhibitor cocktail from Nacalai Tesque (Kyoto, Japan). Fetal bovine serum (FBS) was purchased from Biowest (Nuaillé, France). N-acetyl-L-cysteine (NAC) was purchased from Sigma Aldrich (St. Louis, USA). All biochemicals used in this research were of the highest purity available.

2.2. Cells and cell cultures

The HEK293 human embryonic kidney cell line was kindly provided by SBI Pharma Co., Ltd., Tokyo, Japan. The MKN45 human gastric cell line was purchased from Riken BRC, Ibaraki, Japan. The PC-3 human prostate cancer cell line was provided by Dr. Inoue, Kochi University, Kochi, Japan. All cells were maintained in RPMI-1640 medium supplemented with 10% (v/v) FBS and 1% (v/v) ABAM. Cells were cultured under an atmosphere containing 5% CO_2 and at 37 ˚C.

2.3. Cell irradiation

Cells were incubated with 1-mM ALA under an atmosphere containing 5% CO_2 and 37 ˚C for 4 h and exposed to light-emitting diode (LED) irradiation for 5 min (635 nm) by placing the plate below an LED irradiation unit (provided by SBI Pharma Co., Ltd., Tokyo, Japan) according to the method described in a previous study [7]. Cells were further incubated in the dark for 24 h, and their viability was then measured using an MTT assay according to the method described in a previous study [13].

2.4. Expression analysis after photoirradiation

Total cellular RNA was purified using a NucleoSpin RNA II kit (MACHEREY-NAGEL, Düren, Mannheim, Germany). Further, cDNA was generated by reverse transcription using a PrimeScript RT reagent kit with gDNA Eraser (Takara Bio Inc., Shiga, Japan). We assessed cell cycle-related gene expression using the PrimerArray Cell cycle (Human) kit (Takara Bio Inc.). PrimerArray results were analyzed using PrimerArray Analysis Tool Ver.2.2 (Takara Bio Inc.). All procedures were performed according to the manufacturers' instructions. Genes with differences greater than 2-fold and lesser than 0.5-fold are summarized.

2.5. Quantitative polymerase chain reaction

Further, cDNA was generated using the same method described as described above. A Thermal Cycler Dice Real Time System (Takara Bio Inc., Shiga, Japan) was used for a two-step reverse transcription polymerase chain reaction. The transcripts were quantified using SYBR Premix ExTaq (Takara Bio Inc., Shiga, Japan). The primers used were as follows:

Heme oxygenase 1 (HO-1) primers: forward, 5′-GCTCAAAAAGATT GCCCAGAA-3′; reverse, 5′-TCACATGGCATAAAGCCCTACA-3′

PAI-1 primers: forward, 5′-GCATGACCTACCAGGACAGAACT-3′; reverse, 5′-TCCGAGCTGCCTGTCTCTCT-3′

P21 primers: forward, 5′-GCAGACCAGCATGACAGATTT-3′; reverse, 5′-GGATTAGGGCTTCCTCTTGGA-3′

β-actin primers, forward, 5′-TGGCACCCAGCACAATGAA-3′; reverse, 5′-CTAAGTCATAGTCCGCCTAGAAGCA-3′

The amplification conditions included 30 s at 95 ˚C, 45 cycles of 95 ˚C for 5 s, and 60 ˚C for 60 s, followed by dissociation for 15 s at 95 ˚C and 30 s at 60 ˚C and then 15 s at 95 ˚C. The Thermal Cycler Dice Real Time System analysis software (Takara Bio Inc., Shiga, Japan) was used to analyze the data. Ct values (cycle threshold) were calculated using the crossing-point method, and the relative quantities of target mRNA were determined by comparison with a standard curve. The results for each sample were normalized to the housekeeping gene β-actin.

2.6. Western blot analyses

Western blot analyses were performed as described previously [14]. Primary antibodies used were as follows: anti-p21 (sc-397, 1:200 dilution, Santa Cruz Biotechnology, Texas, United States), anti-Ki-67 (ab15580, 1:1000 dilution, Abcam, Cambridge, Great Britain), and anti-actin (691001, 1:500 dilution, MP Biomedicals, Santa Ana, United States). Furthermore, secondary antibodies used were anti-mouse and -rabbit IgG HRP-conjugated antibody (1:3000 dilution, Cell Signaling Technology, Beverly, United States).

2.7. Cell proliferation assay

Cells were trypsinized and collected every 24 h post- photoirradiation. Cells were exposed to trypan blue and the number of unstained cells was counted.

2.8. HPLC analysis of PpIX

Cells were incubated with 1 mM ALA under 5% CO2 at 37 ˚C in the dark for 24 h. High-performance liquid chromatography (HPLC) analysis was performed as previously described with some modifications [5]. Cells were washed and lysed using 0.1 M NaOH, and lysates were extracted by addition of three volumes of DMF/2-propanol (100:1, v/v). Mixtures were then centrifuged to remove proteins, and supernatants were incubated at room temperature in the dark for 1 day. Then, 100 μ L aliquots were collected, and porphyrins were separated using an HPLC system (Type Prominence, Shimadzu, Kyoto, Japan) equipped with a reversed-phase C18 column (CAPCELLPAK, C18, SG300, 5 μ m, 4.6 mm × 250 mm; SHISEIDO, Tokyo, Japan) maintained at 40 ˚C. Elution solvent A contained 1 M ammonium acetate and 12.5% acetonitrile (pH 5.2), and solvent B contained 50 mM ammonium acetate and 80% acetonitrile (pH 5.2). Porphyrins were eluted with solvent A for 5 min, with a linear gradient of solvent B (0–100%) for 25 min and then with solvent B for 10 min. Flow was maintained at a constant rate of 1.0 mL/min, and porphyrins were continuously detected using a fluorospectrometer (excitation at 404 nm, detection at 624 nm). Porphyrin concentrations were estimated using calibration

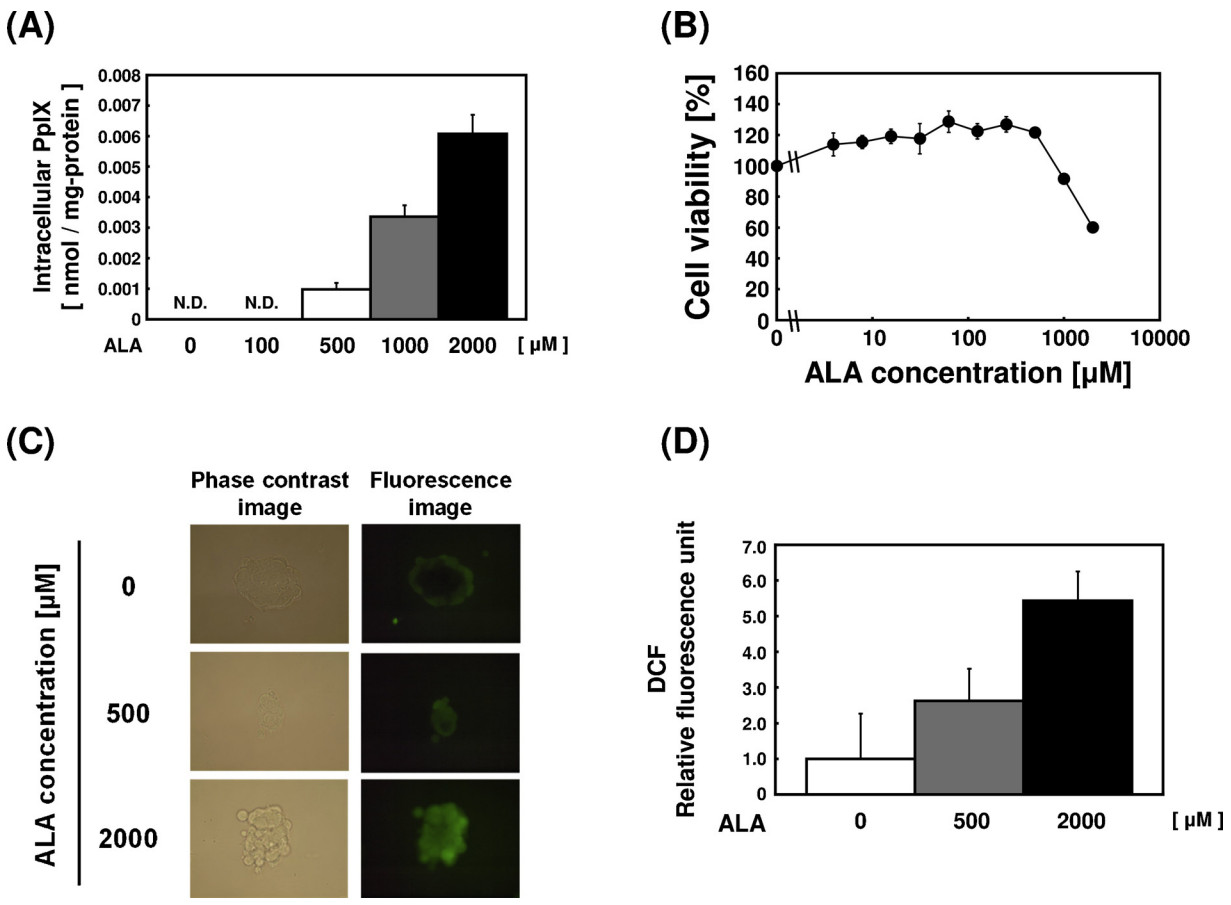

Fig. 1. 5-Aminolevulinic acid (ALA)-induced protoporphyrin IX (PpIX) accumulation and reactive oxygen species (ROS) production in HEK293 cells. Cells were treated with ALA at different concentrations for 4 h and irradiated at 635 nm for 5 min, and the power was optimized to 1803 mJ/cm^2 (b–d). (a) PpIX accumulation at different ALA concentrations. Protein was quantified using the Bradford method (n = 3). (b) Photoirradiation at several ALA concentrations. Culture medium was changed prior to photoirradiation (n = 6). (c) Dichlorofluorescein (DCF) fluorescence images after photoirradiation. (d) DCF fluorescence intensity after photoirradiation. Excitation = 480 nm, emission = 522 nm; n = 3. Bars represent standard deviation (SD).

curves from porphyrin standards.

2.9. Statistical analysis

For statistical evaluation of data and graph preparation, Microsoft Office Excel software was used. The unpaired two tailed *t*-test was applied to test significance of differences between groups of data. The data are expressed as averages from at least two independent measurements ± standard deviation (S.D.).

3. Results

3.1. Photoirradiation induces ROS formation in HEK293 cells

This study aimed to examine the effects of photoirradiation on cell proliferation and gene expression. First, we confirmed the functionality of our photoirradiation experimental system by determining whether photoirradiation-induced ROS production could be detected in HEK293 cells. Cells treated with 0–2000 μM of ALA for 4 h exhibited PpIX accumulation in an ALA concentration-dependent manner (Fig. 1a). PpIX accumulation was detected at ALA concentrations > 500 μM, and this result correlated with photoirradiation cytotoxicity (Fig. 1b). Dichlorodihydro-fluorescein (DCHF)-diacetate is metabolized to DCFH by esterases in the cytoplasm. When DCFH reacts with ROS, it is converted to dichlorofluorescein, which is fluorescent. ALA-treated cells exhibited DCF-specific fluorescence in an ALA concentration-dependent manner (Fig. 1c, d). These results validated that the photoirradiation system was suitable for use in the remaining study.

3.2. HO-1 and p21 expression upregulated after photoirradiation

HO-1 is a heme-degrading enzyme, and its expression increases when intracellular heme levels increase [15]and when ROS is present [16]. Physiologically, this is considered to occur because biliverdin, the heme degradation product formed by HO-1, is an antioxidant [17,18]. HO-1 expression increased three-fold after ALA treatment regardless of photoirradiation (Fig. 2a). This suggests that intracellular heme was accumulated in ALA-treated cells, thus inducing HO-1 production. Furthermore, its increased expression was observed in after photoirradiation for 120 min. In addition, the expression of PAI-1, which is a well-known ROS production marker [19] was induced by irradiation (Fig. 2b). PAI-1 upregulation was suppressed by NAC, an ROS scavenger. Interestingly, p21 gene expression was induced in the photoirradiation group (Fig. 2c). These results suggest that ROS production by photoirradiation alters gene expression and that photoirradiation may repress cell proliferation because p21 controls the cell cycle transition from G1 to S phase [20,21]. Therefore, we investigated cell proliferation in cancer cells after photoirradiation.

3.3. Optimization of conditions for photoirradiation of cancer cells

To investigate post-photoirradiation effects on cancer cells, we first optimized suitable systems for PC-3 and MKN45 cancer cells. Because these cancer cells accumulate much higher levels of PpIX than HEK293

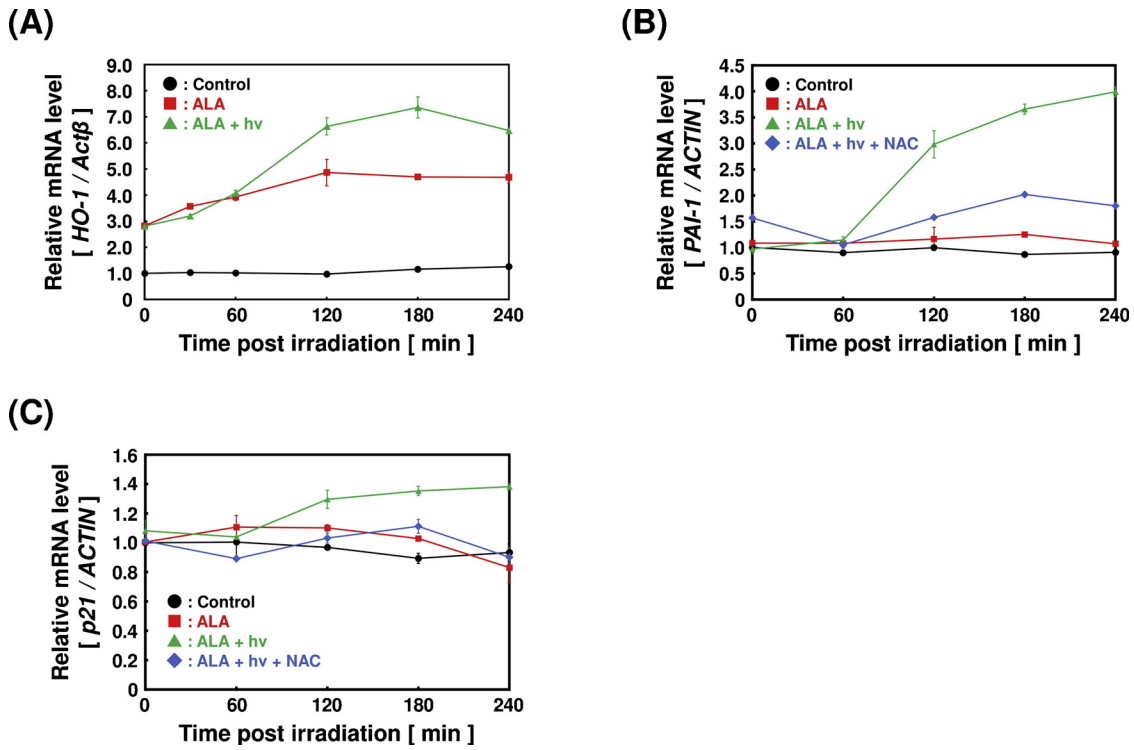

Fig. 2. Gene expression changes in HEK293 cells after photoirradiation. Cells were treated with 500-μM ALA for 4 h before photoirradiation at 635 nm for 5 min, and the power was optimized to 1803 mJ/cm^2. NAC was used at 10 mM, and controls were not treated with ALA or photoirradiation. All gene expressions were normalized to β-actin. (a) HO-1. (b) PAI-1 and (c) p21 expressions (n = 2). Bars represent standard deviation (SD).

cells [5,7], they are more sensitive to photoirradiation cytotoxicity. We previously identified that cell density or dormancy both critically affect PpIX accumulation and cellular responses to photoirradiation [5]. Therefore, in this study, we assessed both photoirradiation power and cell density in the two cancer cell lines prior to further analysis. Fig. 3a demonstrates the effect of the same photoirradiation treatment used in HEK293 cells (Fig. 1b) in PC-3 and MKN45 cancer cells. Because almost 60% of the cancer cells underwent cell death at 1-mM ALA, we reduced both light power and cell density (Fig. 3b-e, Supplementary Fig. 1a-d). Accordingly, the cell density and light power were optimized to Table. 1 described respectively because almost no cell death was observed under these conditions.

3.4. Summarizes the primer array analysis in PC-3 cells post–photoirradiation, suggesting the repression of cell proliferation

To analyze changes in whole gene regulation after photoirradiation, we performed primer array analysis in PC-3 cells. Genes with differences greater than 2-fold and lesser than 0.5-fold are summarized. CDKN2B (p15), CDKN2C (p18), and CDKN2D (p19) were upregulated in the photoirradiation-treated cells compared with those in the untreated control or ALA-treated group (Table 2, Supplementary Fig. 2a-b). These genes inhibit CDK4 and/or CDK6, which control the cell cycle transition from G1 to S phase [22]. In addition, SMAD4 and TGFB1 were upregulated in the photoirradiation group. SMAD4, TGFB1, and TGFB2 are the main factors involved in the TGF-B/SMAD signaling pathway [23]. This pathway controls the expression of several genes involved in G1/S arrest; thus, their activation suppresses cell proliferation. CDC25A is a CDK phosphatase that activates cell cycle turnover [24–26]. This expression was decreased in both untreated control and ALA-treated group. Therefore, photoirradiation may suppress cancer cell proliferation through several signal pathways.

3.5. p21 upregulation and Ki-67 downregulation after photoirradiation

Further, we focused on the cell proliferation markers p21 and Ki-67, and examined time-dependent expression changes in PC-3 and MKN45 cells. We observed that p21 mRNA expression was upregulated in the photo-irradiated group in both cell lines; however, this was not observed in the only ALA-treated group (Fig. 4a, b). Protein level analysis in PC-3 cells showed that p21 upregulation continued for 48 h (Fig. 4c). Accordingly, p21 upregulation resulted in Ki-67 downregulation after photoirradiation (Fig. 4d). These results are consistent with the primer array results and indicate the suppression of cancer cell proliferation.

3.6. Photoirradiation suppresses cancer cell proliferation

To confirm the suppression of cell proliferation, we counted cell numbers post-photoirradiation up to 5 days. Cells were treated with ALA and photoirradiation as described in Table 1, stained with trypan blue, and the negative cells were counted. The photo-irradiated group exhibited lower cell proliferation than the control or ALA-treated groups in both PC-3 and MKN45 cells (Figs. 5a and b). These results strongly suggest that the proliferation of cancer cells that survive photoirradiation is suppressed. In clinical aspects, surface tumors undergo cell death through ROS-induced apoptosis or necrosis after photoirradiation. Although deep tumors do not immediately undergo cell death after photoirradiation, their proliferation may be suppressed (Fig. 6).

4. Discussion

Photoirradiation after ALA treatment is an innovative technology for both diagnosis and therapy of cancer. Current studies particularly focus on ALA-PDT, which has the advantages of minimal invasiveness, superior aesthetic outcome, low morbidity, minimal functional disturbance, good tolerance, and the ability to be used repeatedly at the

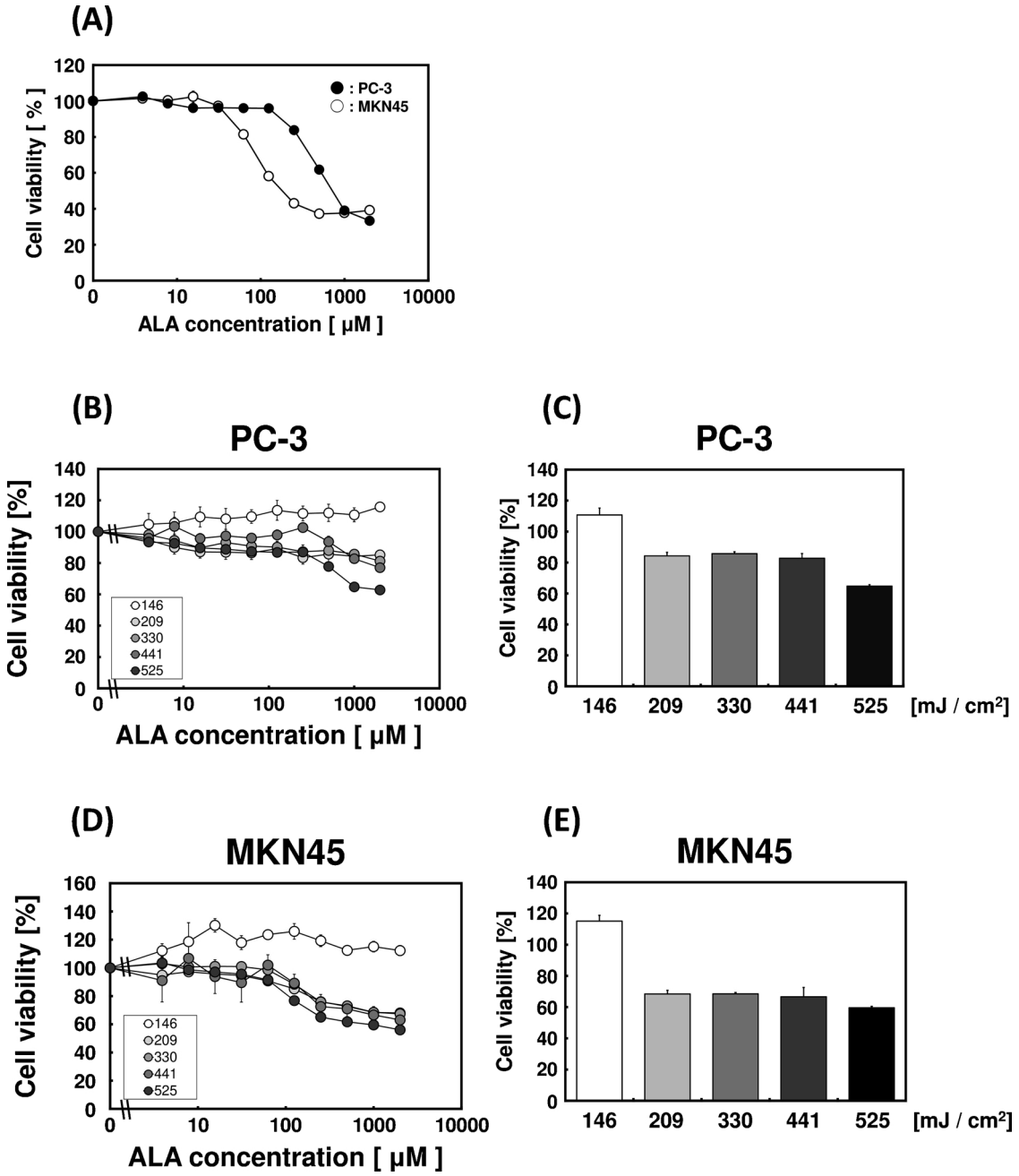

Fig. 3. Effects of photoirradiation power and cell density in PC-3 and MKN45 cells. Cells were treated with different concentrations of ALA for 4 h and irradiated with 635 nm light for 5 min at various powers. Cell density was optimized to 5.0×10^5 cells/35-mm dish in all experiments. (a) Photoirradiation was optimized to 1803 mJ/cm^2. (b) ALA and photoirradiation optimization in PC-3 cells. (c) Light power optimization in PC-3 cells with 1-mM ALA. (d) ALA and photoirradiation optimization in MKN45 cells. (e) Light power optimization in MKN45 cells with 1-mM ALA (n = 6). Bars represent standard deviation (SD).

Table 1
Photoirradiation conditions in cancer cells for further research. A cell density of 5.0×10^5 cells/35-mm dish was used for gene expression analysis, and that of 5.0×10^4 cells/35-mm dish was used for the cell proliferation assay.

	5.0×10^5	5.0×10^4	[cells / 35-mm dish]
MKN45	146	209	[mJ / cm^2]
PC-3	146	330	
	1mM ALA 4 hours for all cell		

same site [27]. Various reports have described the effects of ALA-PDT on the cancer cell death, and we previously reported regarding its effects on gastric [7], bladder [28], and prostate cancer cells [5]. Furthermore, a recent report has described its effect on ovarian clear-cell carcinoma [29]. Therefore, ALA-PDT is reported to be effective in inducing rapid cell death in several tumors. In addition, a recent study suggested that ALA-PDT-treated tumor cells can stimulate dendritic cell maturation [30]. However, few reports have focused on the changes in gene expression induced by photoirradiation.

In this study, we first showed that photoirradiation increases ROS production in an ALA-concentration dependent manner, which in turn upregulates the expression of three genes in HEK293 cells. HO-1, PAI-1, and p21 mRNA expression was upregulated after photoirradiation; however, the effect was abrogated by adding the ROS scavenger NAC. Previous research has reported that ALA-PDT-treated cancer cells increase both HO-1 mRNA and protein expression [31]. Another study

Table 2
Primer array results in PC-3 cells. Cells were treated with 1-mM ALA for 4 h followed by photoirradiation at 635 nm for 5 min, and the power is optimized to 146 mJ/cm in the photoirradiation group. All gene expressions were normalized to β-actin. Genes with differences greater than 2-fold and lesser than 0.5-fold are summarized here (n = 1).

	ALA + hν vs. Control	ALA + hν vs. ALA
ATM	–	UP
CDKN2B (p15)	UP	UP
CDKN2C (p18)	UP	UP
CDKN2D (p19)	UP	UP
TP53 (p53)	–	UP
SMC1A	–	UP
SMAD4	UP	UP
CDC25A	DOWN	DOWN
MAD1L1	UP	–
WEE1	–	UP
TGFB1	UP	UP
TGFB2	DOWN	DOWN
TGFB3	–	UP

reported that HO-1 increases p21 expression, resulting in cell cycle arrest at the G0/G1 phase [32]. These two reports are consistent with our results in HEK293. Further, we constructed a weak photoirradiation system with low irradiation doses to study the cancer cells that survive irradiation *in vitro* (Fig. 3). Using primer array analysis, we showed that the expressions of several genes that repress cell proliferation are upregulated by photoirradiation of PC-3 cells. Furthermore, p21 and Ki-67 expression was upregulated in both PC-3 and MKN45 cells. Finally, we demonstrated that cell proliferation after photoirradiation is suppressed in both types of cancer cells. To our best knowledge, this is the first report to describe cell proliferation of cancer cells after ALA treatment and photoirradiation, and it suggests that photoirradiation of cancer cells using ALA-PDD or ALA-PDT exhibit suppressed cell proliferation.

Although we showed that photoirradiation-induced ROS alters the expression of several genes, we did not identify the ROS type that is involved in these changes. Singlet oxygen is a major ROS generated by photoirradiation, although other types, such as hydroxy radicals or hydrogen peroxide can be concurrently generated. We demonstrated that NAC treatment prevents these mRNA expression changes; however, NAC is a precursor of glutathione, which can scavenge various types of ROS [33]. In addition, ROS stress will exhibit not only cellular stress but also respective contribution for cell growth. Previous research has reported low ROS promoted cell growth rate [34,35]. We also confirmed cell viability after ALA treatment with weak light irradiation was promoted in Fig. 3. Therefore, future studies are required to clarify the mechanisms, pathways and ROS amount involved using specific ROS scavengers or generators.

According to other reports, cancer cells that survive ALA-PDT exhibit favorable prognostic phenotypes. Tsai et al. reported that ALA-PDT decreases invasion by carcinoma cells (CL1-5 lung adenocarcinoma, A375 melanoma, and MDA-MB-231 breast carcinoma cells) [36]. Furthermore, they suggested that EGFR protein levels are downregulated during ALA-PDT in a cycle- and light-dose-dependent manner. Xie et al. reported that VEGF protein expression by CNE2 nasopharyngeal carcinoma cells is downregulated 14 days after ALA-PDT *in vivo* [37]. Yu and Yu reported that ALA-PDT impairs tumor initiation and chemoresistance in head and neck cancer cells (HNC cells) because the mRNA expression of known cancer stem cell markers, including

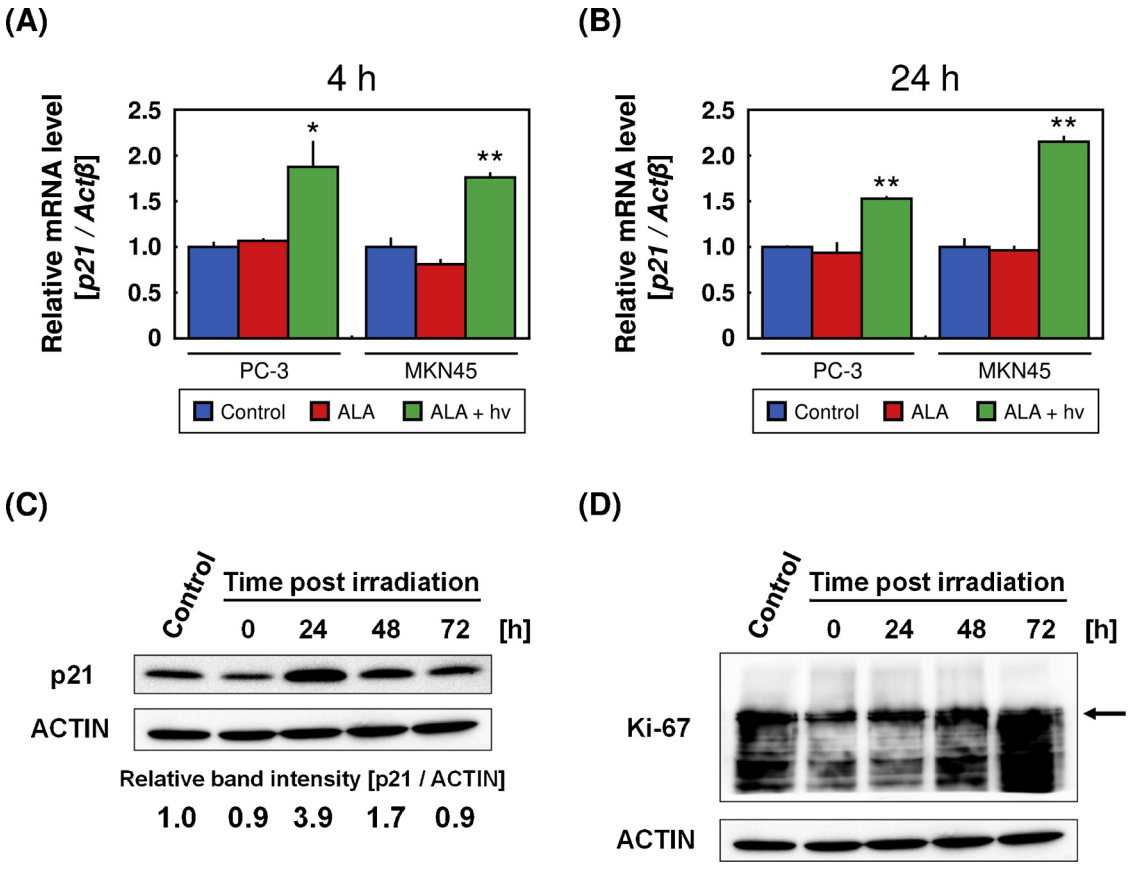

Fig. 4. p21 and Ki-67 expression analysis after ALA treatment. Cells were treated with 1-mM ALA for 4 h followed by photoirradiation for 5 min at 635 nm and the power is optimized to 146 mJ/cm^2 for mRNA or 330 mJ/cm^2 for protein analysis. All gene expressions were normalized to β-actin. (a) p21 mRNA expression at 4 h after photoirradiation (n = 2). (b) p21 mRNA expression at 24 h after photoirradiation (n = 2). (c) p21 protein expression analysis by Western blotting. (d) Ki-67 protein expression analysis by Western blotting. *p < 0.05. **p < 0.01. Bars represent standard deviation (SD).

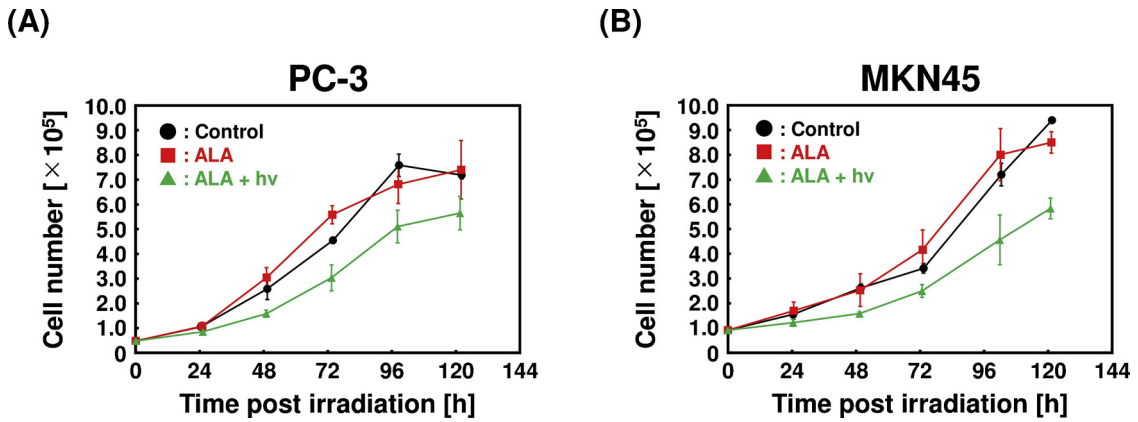

Fig. 5. Cell proliferation after photoirradiation. Cells were treated with 1-mM ALA for 4 h before photoirradiation at 635 nm for 5 min according to the light power described in Table 1. Trypan blue-negative cells were counted over 5 days. (a) PC-3 cells. (b) MKN45 cells (n = 3). Bars represent standard deviation (SD).

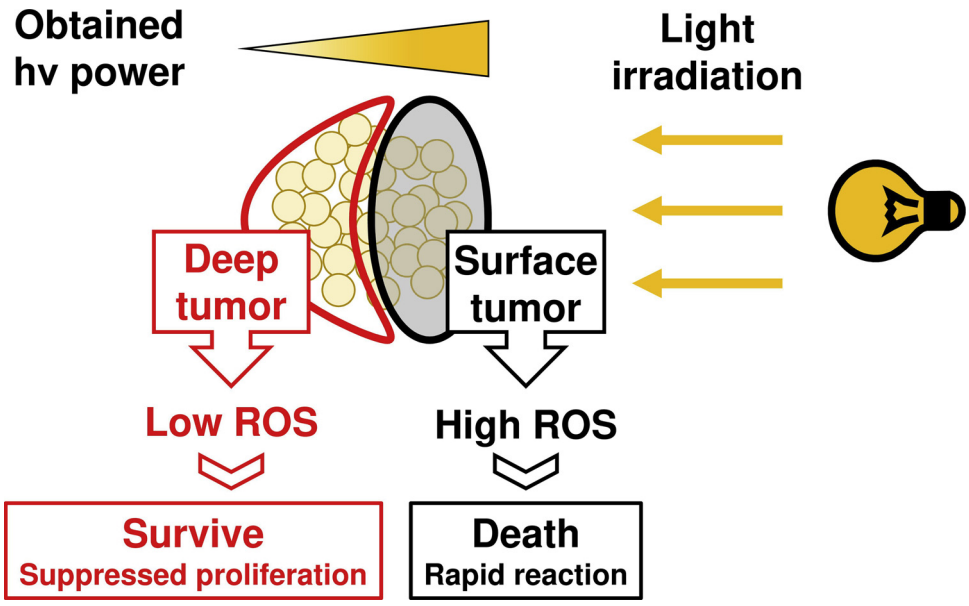

Fig. 6. ALA-PDT irradiation model of solid tumors.

ALDH1, Oct4, and Nanog, was downregulated, rendering HNC cells sensitive to cisplatin and 5-FU drug treatment [38]. Overall, our observations strongly suggest that ALA-PDT has the potential to cause rapid ROS-induced cell death and decrease long-term recurrence rates.

In conclusion, this preliminary study demonstrated that the proliferation of cancer cells that survive photoirradiation can be suppressed in PC-3 and MKN45 cancer cells. This research suggests that photoirradiation using ALA-PDD or ALA-PDT has the potential to delay the proliferation of surviving cancer cells. Additional studies with larger sample sizes are required to validate these findings prior to clinical application.

Funding

The studies in the authors' laboratories were supported by the Grant-in-Aid for Scientific Research (C) (No. 18K05332) from the Ministry of Education, Culture, Sports, Science and Technology.

Declaration of Competing Interest

SBI Pharma CO., Ltd., provided support in the form of salaries for M.N. and T.T., but did not have any additional role in the study design, data collection and analysis, decision to publish or preparation of the manuscript.

Acknowledgement

We thank Mr. Yoshiki Oshimo (Kochi Medical School) for figure modification, Dr. Shinkuro Yamamoto (Graduate student, Kochi Medical School) for clinical discussion, and Mrs. Chiaki Kawada (Kochi Medical School) for laboratory assistance.

Appendix A. Supplementary data

Supplementary material related to this article can be found, in the online version, at doi:https://doi.org/10.1016/j.pdpdt.2019.07.021.

References

[1] I. Ōkura, T. Tanaka, Aminolevulinic acid: Science, Technology and Application, Esubiaiarapuromo (2011).
[2] K. Tabata, S. Ogura, I. Okura, Photodynamic efficiency of protoporphyrin IX: comparison of endogenous protoporphyrin IX induced by 5-Aminolevulinic acid and exogenous porphyrin IX, Photochem. Photobiol. 66 (1997) 842–846, https://doi.org/10.1111/j.1751-1097.1997.tb03235.x.
[3] J.C. Kennedy, R.H. Pottier, Endogenous protoporphyrin IX, a clinically useful photosensitizer for photodynamic therapy, J. Photochem. Photobiol. B 14 (1992) 275–292 (accessed April 4, 2019), http://www.ncbi.nlm.nih.gov/pubmed/

1403373.
[4] B. Krammer, K. Plaetzer, ALA and its clinical impact, from bench to bedside, Photochem. Photobiol. Sci. 7 (2008) 283–289, https://doi.org/10.1039/B712847A.
[5] T. Nakayama, S. Otsuka, T. Kobayashi, H. Okajima, K. Matsumoto, Y. Hagiya, K. Inoue, T. Shuin, M. Nakajima, T. Tanaka, S. Ogura, Dormant cancer cells accumulate high protoporphyrin IX levels and are sensitive to 5-aminolevulinic acid-based photodynamic therapy, Sci. Rep. 6 (2016) 36478, https://doi.org/10.1038/srep36478.
[6] K. Matsumoto, Y. Hagiya, Y. Endo, M. Nakajima, M. Ishizuka, T. Tanaka, S. Ogura, Effects of plasma membrane ABCB6 on 5-aminolevulinic acid (ALA)-induced porphyrin accumulation in vitro: tumor cell response to hypoxia, Photodiagnosis Photodyn. Ther. 12 (2015) 45–51, https://doi.org/10.1016/j.pdpdt.2014.12.008.
[7] Y. Hagiya, Y. Endo, Y. Yonemura, K. Takahashi, M. Ishizuka, F. Abe, T. Tanaka, I. Okura, M. Nakajima, T. Ishikawa, S. Ogura, Pivotal roles of peptide transporter PEPT1 and ATP-binding cassette (ABC) transporter ABCG2 in 5-aminolevulinic acid (ALA)-based photocytotoxicity of gastric cancer cells in vitro, Photodiagnosis Photodyn. Ther. 9 (2012) 204–214, https://doi.org/10.1016/j.pdpdt.2011.12.004.
[8] B. Noodt, K. Berg, T. Stokke, Q. Peng, J. Nesland, Apoptosis and necrosis induced with light and 5-aminolaevulinic acid-derived protoporphyrin IX, Br. J. Cancer 74 (1996) 22–29, https://doi.org/10.1038/bjc.1996.310.
[9] N.L. Oleinick, R.L. Morris, I. Belichenko, The role of apoptosis in response to photodynamic therapy: what, where, why, and how, Photochem. Photobiol. Sci. 1 (2002) 1–21, https://doi.org/10.1039/b108586g.
[10] H.T. Ji, L.T. Chien, Y.H. Lin, H.F. Chien, C.T. Chen, 5-ALA mediated photodynamic therapy induces autophagic cell death via AMP-activated protein kinase, Mol. Cancer 9 (2010) 91, https://doi.org/10.1186/1476-4598-9-91.
[11] K. Inoue, T. Karashima, M. Kamada, A. Kurabayashi, Y. Ohtsuki, T. Shuin, Clinical experience with intravesical instillations of 5-aminolevulinic acid (5-ALA) for the photodynamic diagnosis using fluorescence cystoscopy for bladder cancer, Hinyokika Gakkai Zasshi 97 (2006) 719–729, https://doi.org/10.5980/JPNJUROL1989.97.719.
[12] K. Inoue, H. Fukuhara, T. Shimamoto, M. Kamada, T. Iiyama, M. Miyamura, A. Kurabayashi, M. Furihata, M. Tanimura, H. Watanabe, T. Shuin, Comparison between intravesical and oral administration of 5-aminolevulinic acid in the clinical benefit of photodynamic diagnosis for nonmuscle invasive bladder cancer, Cancer. 118 (2012) 1062–1074, https://doi.org/10.1002/cncr.26378.
[13] K. Inoue, U. Ota, M. Ishizuka, C. Kawada, H. Fukuhara, T. Shuin, I. Okura, T. Tanaka, S. Ogura, Porphyrins as urinary biomarkers for bladder cancer after 5-aminolevulinic acid (ALA) administration: the potential of photodynamic screening for tumors, Photodiagnosis Photodyn. Ther. 10 (2013) 484–489, https://doi.org/10.1016/j.pdpdt.2013.05.002.
[14] Y. Hagiya, T. Adachi, S. Ogura, R. An, A. Tamura, H. Nakagawa, I. Okura, T. Mochizuki, T. Ishikawa, Nrf2-dependent induction of human ABC transporter ABCG2 and heme oxygenase-1 in HepG2 cells by photoactivation of porphyrins: biochemical implications for cancer cell response to photodynamic therapy, J. Exp. Ther. Oncol. 7 (2008) 153–167 (accessed April 4, 2019), http://www.ncbi.nlm.nih.gov/pubmed/18771089.
[15] J. Alam, S. Shibaharas, A. Smith5, Transcriptional Activation of the Heme Oxygenase Gene by Heme and Cadmium in Mouse Hepatoma Cells*, (1989) (accessed April 4, 2019), http://www.jbc.org/content/264/11/6371.full.pdf.
[16] Y. Lavrovsky, M.L. Schwartzman, R.D. Levere, A. Kappas, N.G. Abraham, Identification of binding sites for transcription factors NF-kappa B and AP-2 in the promoter region of the human heme oxygenase 1 gene, Proc. Natl. Acad. Sci. U. S. A. 91 (1994) 5987–5991, https://doi.org/10.1073/PNAS.91.13.5987.
[17] J. Kapitulnik, F.J. Gonzalez, Bilirubin: an endogenous product of heme degradation with both cytotoxic and cytoprotective properties, Mol. Pharmacol. 66 (2004) 773–779, https://doi.org/10.1124/mol.104.002832.
[18] P. Di Mascio, T.P. Devasagayam, S. Kaiser, H. Sies, Carotenoids, tocopherols and thiols as biological singlet molecular oxygen quenchers, Biochem. Soc. Trans. 18 (1990) 1054–1056, https://doi.org/10.1042/BST0181054.
[19] A. Görlach, U. Berchner-Pfannschmidt, C. Wotzlaw, R. Cool, J. Fandrey, H. Acker, K. Jungermann, T. Kietzmann, Reactive oxygen species modulate HIF-1 mediated PAI-1 expression: involvement of the GTPase Rac1, Thromb. Haemost. 89 (2003) 926–935, https://doi.org/10.1055/s-0037-1613480.
[20] J. Wade Harper, G.R. Adami, N. Wei, K. Keyomarsi, S.J. Elledge, The p21 Cdk-interacting protein Cip1 is a potent inhibitor of G1 cyclin-dependent kinases, Cell. 75 (1993) 805–816, https://doi.org/10.1016/0092-8674(93)90499-G.
[21] C. Deng, P. Zhang, J. Wade Harper, S.J. Elledge, P. Leder, Mice lacking p21CIP1/WAF1 undergo normal development, but are defective in G1 checkpoint control, Cell. 82 (1995) 675–684, https://doi.org/10.1016/0092-8674(95)90039-X.
[22] H. Drexler, Review of alterations of the cyclin-dependent kinase inhibitor INK4 family genes p15, p16, p18 and p19 in human leukemia–lymphoma cells, Leukemia. 12 (1998) 845–859, https://doi.org/10.1038/sj.leu.2401043.
[23] Y. Shi, J. Massagué, Mechanisms of TGF-β signaling from cell membrane to the nucleus, Cell. 113 (2003) 685–700, https://doi.org/10.1016/S0092-8674(03)00432-X.
[24] N. Mailand, A.V. Podtelejnikov, A. Groth, M. Mann, J. Bartek, J. Lukas, Regulation of G(2)/M events by Cdc25A through phosphorylation-dependent modulation of its stability, EMBO J. 21 (2002) 5911–5920, https://doi.org/10.1093/EMBOJ/CDF567.
[25] Z. Xiao, Z. Chen, A.H. Gunasekera, T.J. Sowin, S.H. Rosenberg, S. Fesik, H. Zhang, Chk1 mediates S and G2 arrests through Cdc25A degradation in response to DNA-damaging agents, J. Biol. Chem. 278 (2003) 21767–21773, https://doi.org/10.1074/jbc.M300229200.
[26] S. Jinno', K. Sutol, A. Nagata1, M. Igarashi2, Y. Kanaoka1, H. Nojima1, H. Okayama1, Cdc25A Is a Novel Phosphatase Functioning Early in the Cell Cycle, (1994) https://www.ncbi.nlm.nih.gov/pmc/articles/PMC394984/pdf/emboj00055-0063.pdf.
[27] L. Shi, X. Wang, F. Zhao, H. Luan, Q. Tu, Z. Huang, H. Wang, H. Wang, In vitro evaluation of 5-aminolevulinic acid (ALA) loaded PLGA nanoparticles, Int. J. Nanomedicine 8 (2013) 2669–2676, https://doi.org/10.2147/IJN.S45821.
[28] K. Inoue, S. Anai, K. Fujimoto, Y. Hirao, H. Furuse, F. Kai, S. Ozono, T. Hara, H. Matsuyama, M. Oyama, M. Ueno, H. Fukuhara, M. Narukawa, T. Shuin, Oral 5-aminolevulinic acid mediated photodynamic diagnosis using fluorescence cystoscopy for non-muscle-invasive bladder cancer: a randomized, double-blind, multicentre phase II/III study, Photodiagnosis Photodyn. Ther. 12 (2015) 193–200, https://doi.org/10.1016/j.pdpdt.2015.03.008.
[29] T. Teshigawara, M. Mizuno, T. Ishii, Y. Kitajima, F. Utsumi, J. Sakata, H. Kajiyama, K. Shibata, M. Ishizuka, F. Kikkawa, Novel potential photodynamic therapy strategy using 5-Aminolevulinic acid for ovarian clear-cell carcinoma, Photodiagnosis Photodyn. Ther. 21 (2018) 121–127, https://doi.org/10.1016/J.PDPDT.2017.11.013.
[30] J. Ji, Z. Fan, F. Zhou, X. Wang, L. Shi, H. Zhang, P. Wang, D. Yang, L. Zhang, X. Wang, W.R. Chen, ALA-PDT mediated DC vaccine for skin squamous cell carcinoma, Biophotonics Immune Responses X. 9324 (2015) 93240A, , https://doi.org/10.1117/12.2077932.
[31] A. Sieroń, S. Kwiatek, Twenty years of experience with PDD and PDT in Poland-Review, Photodiagnosis Photodyn. Ther. 6 (2009) 73–78, https://doi.org/10.1016/j.pdpdt.2009.07.003.
[32] P. Inguaggiato, L. Gonzalez-Michaca, A.J. Croatt, J.J. Haggard, J. Alam, K.A. Nath, Cellular overexpression of heme oxygenase-1 up-regulates p21 and confers resistance to apoptosis, Kidney Int. 60 (2001) 2181–2191, https://doi.org/10.1046/j.1523-1755.2001.00046.x.
[33] H. Steiling, B. Munz, S. Werner, M. Brauchle, Different types of ROS-scavenging enzymes are expressed during cutaneous wound repair, Exp. Cell Res. 247 (1999) 484–494, https://doi.org/10.1006/excr.1998.4366.
[34] K. Irani, Oxidant signaling in vascular cell growth, death, and survival, Circ. Res. 87 (2000) 179–183, https://doi.org/10.1161/01.res.87.3.179.
[35] M. Benhar, D. Engelberg, A. Levitzki, ROS, stress-activated kinases and stress signaling in cancer, Mol. Biol. (Mosk.) 3 (2002) 420–425.
[36] T. Tsai, H.T. Ji, P.C. Chiang, R.H. Chou, W.S.W. Chang, C.T. Chen, ALA-PDT results in phenotypic changes and decreased cellular invasion in surviving cancer cells, Lasers Surg. Med. 41 (2009) 305–315, https://doi.org/10.1002/lsm.20761.
[37] Y. Ma, G. Zhang, X. Fu, O. Xia, C. Zhan, L. Li, Z. Wang, B. Wu, Esculetin inhibits cell proliferation through the Ras/ERK1/2 pathway in human colon cancer cells, Oncol. Rep. 25 (2011) 223–230, https://doi.org/10.3892/or.
[38] C.H. Yu, C.C. Yu, Photodynamic therapy with 5-Aminolevulinic acid (ALA) impairs tumor initiating and chemo-resistance property in head and neck cancer-derived cancer stem cells, PLoS One 9 (2014) 1–7, https://doi.org/10.1371/journal.pone.0087129.